Proc. of the Second Intl. Conf. on Advances In Bio-Informatics, Bio-Technology and Environmental Engineering- ABBE 2014.

ISBN: 978-1-63248-053-8 doi: 10.15224/ 978-1-63248-053-8-122

Simulation and optimization of hexavalent chromium adsorption on autohydrolyzed Scots Pine (Pinus Sylvestris) sawdust in batch and fixed-bed systems

Dimitrios Sidiras and Dorothea Politi

***Abstract*—In this work, column kinetics of Cr(VI) adsorption on autohydrolyzed (160-240 ^{o}C, 0-50 min) Scots pine (*Pinus sylvestris L.*) sawdust were simulated, in order to optimize the potential use of this material for wastewater cleaning. The effect of the autohydrolysis time and temperature on the microstructure and the crystallinity of pine sawdust was investigated be means of SEM, FTIR, XRD and BET. The Modified dose response (MDR) adsorption column capacity q_0 increased from 0.6376 to 23.71 mg.g^{-1}, indicating that autohydrolysis treatment at 240 ^{o}C for 50 min optimizes the adsorption behavior of the material.**

***Keywords*—adsorption, autohydrolysis, chromium, sawdust, column**

I. Introduction

Industrialization has been contaminating water resources by discharging heavy metals and color. Adsorption is widely used for removal of metals and color from wastewater. Activated carbon is a common adsorbent for the reclamation of municipal and industrial wastewater. The high cost of activated carbon has prompted research on suitable low-cost adsorbents, currently focusing on the use of low cost commercially available lignocellulosic materials (wood sawdust and agricultural residues) as viable substitutes for activated carbon [1-5].

Heavy metals in the aquatic environment have been of great concern because of discharges increase, their toxicity, and other adverse effects on the receiving water. Some of them are cumulative poisonous capable of being assimilated, stored, and concentrated by organisms that are exposed to low concentrations of these substances for long periods or repeatedly for short periods. Safe and effective cleaning/disposal of wastewater is always a challenging task due to the fact that cost-effective treatment alternatives are not presently available. The industrial wastewater treatment processes include reduction precipitation, ion exchange, electrochemical reduction, evaporation, reverse osmosis, direct precipitation. These methods, involve large exposed liquid surface area and long detention periods. Besides, they need high capital cost and recurring expenses such as chemicals, which are not suitable for small-scale industries [6].

Hexavalent chromium exhibits high toxicity. Industrial sources of Cr(VI) include leather tanning, cooling tower blowdown, plating, electroplating, anodizing baths, rinse waters, etc. The sorption capacities of commercial developed carbons and low-cost alternative sorbents for tri-and hexavalent chromium remediation have been studied my numerous researchers [7], and the mechanisms of adsorption on various adsorbents have been established. Chromium's impact on environmental quality, sources of chromium pollution and toxicological / health effects have been, also, investigated.

More specifically, untreated and pretreated lignocellulosic industrial byproducts and agricultural residues have been employed as adsorbents for hexavalent chromium removal from water. These materials include sawdust [4, 8-10], coir pith [10], oil palm fibre [11], olive bagasse [12], wheat straw carbon [13], barley straw carbon [13], pistachio hull [14], leaf mould [15], wheat bran [16], cotton stalk peel [17], walnut shell [18], walnut hull [19], hazelnut shell [18], almond shell [18], rice bran [20], rice husk [10], soybean hulls [21], eucalyptus bark [22], Tamarindus indica seeds [23], short-chain polyaniline synthesized on jute fiber [24], tea factory waste [25], spent mushroom modified by cationic surfactant [26], and olive stone [27].

Furthermore, since lignocellulosic materials are used in the bioethanol industry as source of sugars [28], the process solid residue can be implemented as adsorbent. Autohydrolysis is frequently used to increase the efficiency of lignocellulosics' enzymatic hydrolysis to sugars [29]. Many industrial byproducts and agricultural residues can be autohydrolyzed for the sugars production [30]. The autohydrolysis solid residue can be efficiently used as adsorbent as it has been proved in the case of some basic dyes [31, 32].

In this work, a low cost adsorbent with high capacity is presented, suitable for the efficient removal of hexavalent chromium from water and wastewater. The adsorbent was produced from autohydrolysis of Scots Pine sawdust. The effect of the autohydrolysis conditions on the microstructure and the crystallinity of pine sawdust was determined using SEM, FTIR, XRD and BET surface area techniques. The column adsorption kinetics of Cr(VI) were used to estimate and compare the adsorption capacity of the untreated and pretreated pine sawdust.

Dimitrios Sidiras
University of Piraeus
Greece

Dorothea Politi
University of Piraeus
Greece

Proc. of the Second Intl. Conf. on Advances In Bio-Informatics, Bio-Technology and Environmental Engineering- ABBE 2014.

ISBN: 978-1-63248-053-8 doi: 10.15224/ 978-1-63248-053-8-122

II. Materials and Methods

A. Material development

The Scots Pine (*Pinus Sylvestris*) sawdust used was obtained from a local furniture manufacturing company, as a suitable source for full-scale/industrial applications. The moisture content of the material when received was 8.7% w/w; after screening, the fraction with particle sizes between 0.2 and 1 mm was isolated. The composition of the raw material was as follows (expressed in % w/w on a dry weight basis): 40.1% cellulose measured as glucan (with 52.5% XRD degree of crystallinity); 28.5% hemicelluloses (16.0% measured as manan, 8.9% measured as xylan and the rest 3.6% measured as arabinan); 27.7% Klason acid-insoluble lignin, 0.2% ash, and 3.5% extractives and other acid soluble components (e.g. acid soluble lignin).

The autohydrolysis process was performed in a 3.75-L batch reactor PARR 4843. The isothermal hydrolysis times were 0, 10, 20, 30, 40 and 50 min (not including the non-isothermal preheating and the cooling time-periods); the reaction was catalyzed by the organic acids produced by the pine sawdust itself during autohydrolysis at a liquid-to-solid ratio of 10:1; the liquid phase volume (water) was 2000 mL and the solid material dose (pine sawdust) was 200 g; stirring speed 150 rpm. The reaction ending temperature values were 160°C, 200°C and 240°C, reached after 42, 62 and 80 min preheating time values, respectively.

B. Column studies

Fixed-bed up-flow adsorber studies were conducted in a 15 cm internal height × 2.5 cm internal diameter stainless steel column. The experimental set-up consisted of one column, fed by a multi-channel peristaltic pump at constant flow rates of 10, 20, 30, 40 mL min^{-1}. The initial constant Cr(VI) concentration was 75.0 mg L^{-1}. Interconnective tubing and fittings were made of polytetrafluoroethylene (PTFE). Effluent samples were analyzed to yield output concentration breakthrough curves.

C. Analytical techniques

The degree of crystallinity of pine sawdust cellulose was measured by X-ray diffraction, according to the Segal et al. method [33]. The powder X-ray diffraction (XRD) patterns of the untreated and the pretreated samples were measured by a SIEMENS D5005 X-Ray Diffractometer using Ni-filtered CuKa (λ=0.154 nm) radiation at 45 kV and 40 mA and continuous scan mode. The XRD patterns were recorded in the scan range 2θ=5-70, at scan rate step=0.04o, dwell time=3 sec, i.e. total scan time approximately 1 h and 30 min.

The quantitative saccharification of the original and the autohydrolyzed material was carried out according to the Saeman et al. [34] technique. The filtrates from the quantitative saccharification were analyzed for glucose, xylose and arabinose using high-performance liquid chromatography (HPLC, Agilent 1200) with Aminex HPX-87H Column, refractive index detector and 5 mM H_2SO_4 in water as the mobile phase in order to estimate the cellulose and hemicelluloses. Finally, the acid-insoluble Klason lignin was determined according to the Tappi T222 om-88 method [34].

The BET (Brunauer, Emmet and Teller) surface area of the original and the pretreated pine sawdust was measured from the N2 adsorption isotherm with a Nova® Surface Area Analyzer (Quantachrome Instruments) in accordance with DIN 66132 [35].

The scanning electron microscope (SEM) used herein was a JEOL JSM-6700F Field Emission Scanning Electron Microscopy. The SEM tests were carried out on Pt coated (5 nm) samples. The magnifications were 7500 and 50000.

Fourier transform infrared (FTIR) spectra were obtained using a spectroscope (MAGNA-IR 750 Spectrometer, Serrie II, Nicolet). The sampling technique used herein was diffuse reflectance. The powder samples were scanned for wavenumber 650-4000 cm^{-1}.

The concentration of Cr(VI) was measured by using a HACH DR4000U UV–visible spectrophotometer, according the Method 8023 (1,5-Diphenylcarbohydrazide Method) HACH DR/4000 PROCEDURE, CHROMIUM, HEXAVALENT.

III. Results and Discussion

A. Autohydrolysis

Cellulose crystallinity, accessible surface area, protection by lignin, and sheathing by hemicelluloses, all contribute to lignocellulosic biomass resistance to autohydrolysis [28-31]. Autohydrolysis of cellulose and hemicelluloses produces glucose, xylose and degradation products as 5-HMF and furfural, respectively. The autohydrolysis is affected by temperature and reaction time. Cellulose fractions are hydrolyzed to water-soluble cellulo-oligosaccharides and glucose, hemicelluloses are hydrolyzed to xylo-oligosaccharides and xylose and acid-insoluble lignin fraction is not affected by autohydrolysis.

The solid residue yield and the composition of the autohydrolyzed pine sawdust (dry weight of product % w/w of the original dry material) are presented in Table I, as a function of autohydrolysis time. The hemicelluloses percentage of the autohydrolyzed pine sawdust was significantly decreased by autohydrolysis intensification.

The cellulose percentage of the pretreated sawdust reached a maximum of 50.3% w/w at 200°C for 50 min. The lignin percentage of the solid residue increased up to 62.4% w/w at 240 °C for 50 min.

B. Microstructure

The SEM micrographs for untreated autohydrolyzed (at 160, 200 and 240 °C for 40 min) pine sawdust are given in Fig. 1. The magnifications were 7500 for Fig. 1a, c, e, g and 50000 for Fig. 1b, d, f, h. The texture of the pretreated materials was rougher than that of the untreated sawdust.

Proc. of the Second Intl. Conf. on Advances In Bio-Informatics, Bio-Technology and Environmental Engineering- ABBE 2014.

ISBN: 978-1-63248-053-8 doi: 10.15224/ 978-1-63248-053-8-122

TABLE I. SOLID RESIDUE YIELD, COMPOSITION AND BET SURFACE AREA OF THE AUTOHYDROLYZED PINE SAWDUST AS A FUNCTION OF THE AUTOHYDROLYSIS TIME AT 160-240 ^{o}C.

Time, t_{ai} (min)	160 ^{o}C	200 ^{o}C	240 ^{o}C
Solid residue yield (% w/w)			
-	100.0	100.0	100.0
0	94.1	80.1	65.4
10	90.7	76.8	60.0
20	88.3	75.0	56.3
30	84.7	72.1	54.7
40	85.6	70.9	45.8
50	83.9	68.5	44.6
Cellulose (% w/w)			
-	40.1	40.1	40.1
0	42.6	48.6	44.2
10	44.2	49.1	44.1
20	45.4	49.2	33.5
30	47.3	49.5	30.1
40	46.9	49.2	22.8
50	47.8	50.3	18.9
Hemicelluloses (% w/w)			
-	28.5	28.5	28.5
0	28.2	10.7	0
10	23.9	5.9	0
20	19.1	2.3	0
30	17.2	1.0	0
40	15.3	0.3	0
50	14.6	0.2	0
Lignin (% w/w)			
-	27.7	27.7	27.7
0	29.9	34.9	42.4
10	31.4	36.6	47.0
20	31.9	37.8	49.6
30	33.1	39.1	51.4
40	33.0	39.8	60.8
50	33.2	40.6	62.4
BET surface area ($m^2 g^{-1}$)			
-	0.894	0.894	0.894
0	2.510	3.622	5.290
10	2.621	3.703	7.011
20	2.802	3.812	10.093
30	2.911	4.023	10.998
40	2.943	4.578	19.075
50	3.055	5.109	19.202

Roughness was increasing by increasing the autohydrolysis severity (e.g. autohydrolysis temperature) as it can be easily observed at magnification 50000. Moreover, the opening of the lignocellulosic structure and the presence of larger pores can be, also, observed. These changes of the lignocellulosic matrix seem reasonable, taking into account that the pretreated material has a high lignin percentage (see Table 1) with more open Klason lignin structure. The rough surface, the open structure and the larger pores of the autohydrolyzed pine sawdust explains its enhanced adsorption properties. In Fig. 2 we present the SEM micrographs for untreated pine sawdust before and after Cr(VI) adsorption. The adsorption conditions were 23 ^{o}C, C_0=75 mg L^{-1}, m/V=4 g L^{-1}, pH=2.0 and agitation speed=300 rpm. The texture of the sawdust after Cr(VI) adsorption seems more rough and shows a higher contrast than before Cr(VI) adsorption. This is more obvious at magnification 50000, and it is obviously due to the adsorption of Cr(VI) on the pine sawdust surface.

C. *Surface Chemistry*

The cell walls of pine sawdust consist mainly of cellulose hemicelluloses, lignin and many hydroxyl groups, such as tannins or other phenolic compounds. Lignin is a polymer material that is built up from the phenyl propane nucleus, an aromatic ring with a three-carbon side chain. Tannins are complex polyhydric phenols that are soluble in water and have the property of precipitating protein. The FTIR spectra of the untreated pine sawdust and the autohydrolyzed at 160, 200 and 240 ^{o}C for 0 and 40 min pine sawdust are given in Fig. 3a. The FTIR spectra of sawdust show that some peaks were shifted. In the case of the untreated pine sawdust, there is a strong peak at wavenumber 3471 cm^{-1} representing the –OH stretching of phenol group of cellulose and lignin, whereas the peaks at 2939 cm^{-1} and 2146 cm^{-1} indicate the presence of $–CH_2$ stretching of aliphatic compound and –NH stretching, respectively. The appearance of peaks at 1741 cm^{-1} and 1612 cm^{-1} imply the presence of C=O stretching of aldehyde group and C=C stretching of phenol group, respectively. The peaks at 1516 cm^{-1} can be due to C=C of aromatic ring. Peaks at 1470 cm^{-1} and 1437 cm^{-1} suggest $–CH_2$ bending and –OH bending, respectively. The peak at 1372 cm^{-1} shows C-O-H bending. Peaks at 1286 cm^{-1} and 1140 cm^{-1} can be due to C–O stretching of phenolic group and six-member cyclic ether group of cellulose, respectively. These wavenumber values are very close to those reported for pine sawdust by Wang et al. [37] and for meranti sawdust by Ahmad *et al.* [38].

In addition, the pretreated with autohydrolysis pine sawdust shows a strong peak shift towards the region 3354-3412 cm^{-1} representing the –OH stretching of phenol group of cellulose and lignin. The peak shift towards the region 2065-2139 cm^{-1} indicates the presence of –NH stretching, whereas the appearance of peak shift towards the region 1701-1738 cm^{-1} indicates the presence of C=O stretching of aldehyde group. The peak shift towards the region 1425-1450 cm^{-1} can be attributed to –OH bending. The peak shift towards the region 1065-1120 cm^{-1} can be due to six member cyclic ether group of cellulose. The new peak at 822 cm^{-1} suggests the presence of aromatic C-H deformation. These shifts observed in the FTIR spectrum imply the changes of the respective functional groups on the surface of autohydrolyzed pine sawdust.

As regards the untreated pine sawdust after Cr(VI) adsorption (23 ^{o}C, C_0=75 mg L^{-1}, m/V=4 g L^{-1}, pH=2.0,

Proc. of the Second Intl. Conf. on Advances In Bio-Informatics, Bio-Technology and Environmental Engineering- ABBE 2014.

ISBN: 978-1-63248-053-8 doi: 10.15224/ 978-1-63248-053-8-122

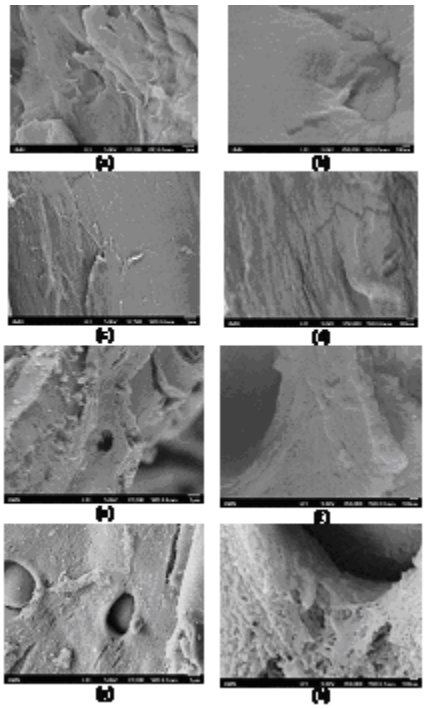

Figure 1. SEM micrographs for untreated (a, b) and autohydrolyzed at 160 ^{o}C (c, d) 200 ^{o}C (e, f) and 240 ^{o}C (g, h) pine sawdust (autohydrolysis isothermal time 40 min).

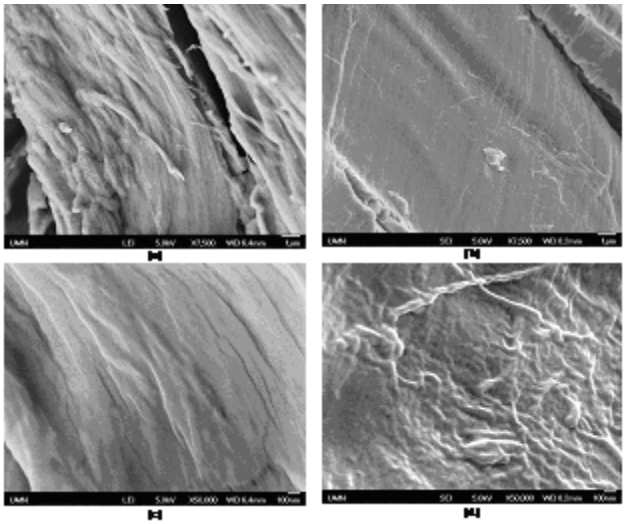

Figure 2. SEM micrographs for untreated pine sawdust before (a, c) and after Cr(VI) adsorption (b, d).

agitation speed=300 rpm), there is a strong peak shift at wavenumber 3386 cm^{-1} representing the –OH stretching of phenol group of cellulose and lignin, and a peak shift at 2904 cm^{-1} indicating the presence of –CH_2 stretching of aliphatic compound (Fig. 3b). The peak shift at 1452 cm^{-1} can be attributed to –CH_2 bending. Peaks shift at 1271 cm^{-1} and 1117 cm^{-1} can be due to C–O stretching of phenolic group and six-member cyclic ether group of cellulose, respectively.

Moreover, a strong peak shift at wavenumber 3417 cm^{-1} appears in the autohydrolyzed (240 ^{o}C, 40 min) pine sawdust

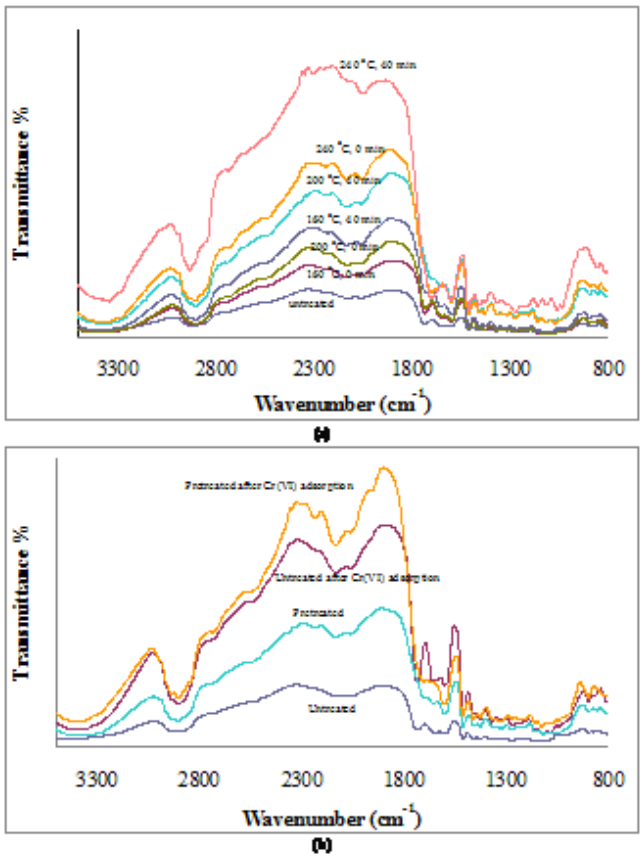

Figure 3. FTIR spectra of (a) untreated and autohydrolyzed at 160, 200 and 240 ^{o}C for 0 and 40 min sawdust, and (b) untreated and autohydrolyzed at 200 ^{o}C for 40 min sawdust before and after Cr(VI) adsorption.

after Cr(VI) adsorption (Fig. 3b), representing the –OH stretching of phenol group of cellulose and lignin, and a peak shifted at 2906 cm^{-1} indicate the presence of –CH_2 stretching of aliphatic compound. The peak shift at 2135 cm^{-1} implies the presence of –NH stretching. The appearance of peak shift at 1593 cm^{-1} shows the presence of C=C stretching of phenol group. The peak shift at 1427 cm^{-1} can be attributed to –OH bending. The peak shift at 1126 cm^{-1} can be due to six-member cyclic ether group of cellulose.

The peak shifts observed in the FTIR spectra of the untreated and autohydrolyzed sawdust before and after Cr(VI) adsorption suggest some changes of functional groups on the surface of the sawdust that can be attributed to bonding with the adsorbed Cr(VI).

D. Crystalline structure

An excellent X-ray diffraction is suitable to analyze the crystallinity of cellulose in wood. Fig. 4 shows the XRD patterns of the untreated pine sawdust and of the autohydrolyzed at 240 ^{o}C for 40 min (+80 min preheating period) pine sawdust. Two broad peaks at the 2θ values of around 16° and 22° for the untreated sawdust were due to the 1 0 1 and 0 0 2 lattice spacing of cellulose in wood [31]. For the autohydrolyzed sawdust, these two peaks became low-height and broad, suggesting structural destruction of crystalline cellulose, in accordance with a sharp weight loss at

Proc. of the Second Intl. Conf. on Advances In Bio-Informatics, Bio-Technology and Environmental Engineering- ABBE 2014.

ISBN: 978-1-63248-053-8 doi: 10.15224/ 978-1-63248-053-8-122

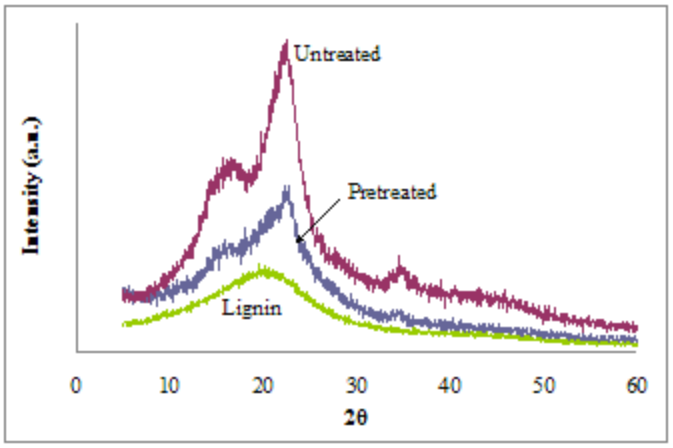

Figure 4. XRD patterns of untreated pine sawdust, autohydrolyzed at 240 oC for 40 min pine sawdust and Klason Lignin produced from untreated sawdust.

these conditions (Table I). The obtained rich-to-lignin material is relatively amorphous. Klason Lignin obtained from the pine sawdust gives a very broad peak at the 2θ value of around 20°. This 2θ value is close to that of amorphous cellulose produced by ball milling.

E. *BET surface area as affected by the autohydrolysis conditions*

The surface area (in $m^2 \cdot g^{-1}$, measured by the BET method) experimental data are given in Table I as a function of the autohydrolysis time at 160-240°C. The effect of autohydrolysis is not significant at 160°C and only moderate at 200°C. The BET surface area is increasing significantly for autohydrolysis at 240°C. The efficient removal of the hemicelluloses and the amorphous part of cellulose results in 'opening' of the pores of the structure of the lignocellulosic matrix [5, 29]. This phenomenon, and the rough texture (see the SEM micrographs in Fig. 1 and 2), increases the BET surface area of the material, which accounts partly for the advanced adsorption properties of the autohydrolyzed sawdust over the untreated one.

F. *Column studies*

For the adsorption column experiments the 'bed depth service model' developed by Bohart and Adams [39] is commonly used as follows

$$\ln\left(\frac{C_i}{C} - 1\right) = \frac{K \cdot N \cdot x}{u} - K \cdot C_i \cdot t \qquad (1)$$

where C=effluent concentration ($mg \cdot L^{-1}$); C_i=influent concentration ($mg \cdot L^{-1}$); K=adsorption rate coefficient ($L \cdot mg^{-1} \cdot min^{-1}$); N=adsorption capacity coefficient ($mg\ L^{-1}$); x=bed depth (cm); u=linear velocity ($cm \cdot min^{-1}$); and t= adsorption time (min).

Robert Clark [40] has developed an alternative to the 'simple logistic function', called the 'generalized logistic function', which incorporates the parameter n of the Freundlich adsorption isotherm:

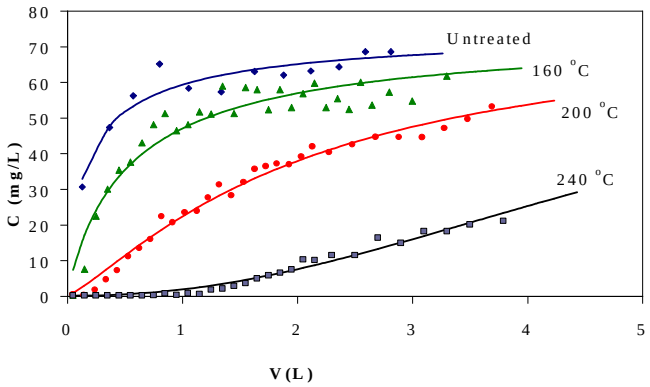

Figure 5. Breakthrough curves for fixed beds of untreated and autohydrolyzed (at 160, 200 and 240 °C for 50 min pine sawdust.)

$$C = \left[\frac{C_i^{\,n-1}}{1 + Ae^{-rt}}\right]^{\frac{1}{n-1}} \qquad (2)$$

where n is the Freundlich isotherm parameter; $A=e^{K.N.x/u}$; $r=K\,C_i$. Transforming and linearizing (2), we obtain:

$$ln\left[\left(\frac{C_i}{C}\right)^{n-1} - 1\right] = ln\ A - r \cdot t \qquad (3)$$

For n=2, we obtain the Bohart–Adams model given by (1), which can be rewritten under the form of the logistic (symmetric sigmoid) model, this expression is reduced to

$$C = \frac{C_i}{1 + Ae^{-rt}} \qquad (4)$$

K, N can be calculated from the equations $K=r/C_i$ and $N=u \cdot lnA/(x \cdot K)=C_i \cdot u \cdot lnA/(x \cdot r)$, while the values of A and r can be estimated by NLRA from the column effluent data (C_i= 75 mgL^{-1} for the cases presented in Fig. 5). The effluent Cr(VI) solution volume V (in L) is $V=Q \cdot t$, where Q is the Cr(VI) solution flow rate, equal to 20 mL min^{-1}. The theoretical estimations sufficiently simulate the experimental data. N was found to be 4744 $mg \cdot L^{-1}$ for the autohydrolyzed pine sawdust (at 240°C for 50 min), i.e., much higher than the N=451 $mg\ L^{-1}$ for the untreated one. In addition, K was found to be 0.000242 L mg^{-1} min^{-1} for the autohydrolysis-treated material, i.e., very close to the K=0.000241 L mg^{-1} min^{-1} for the untreated one. The *SEE*-values are given in Table II. The fitting of the Bohart–Adams model to experimental data was better than the fitting of the Clark model. In general, for autohydrolysis time equal to 50 min, N-value was found to be given by the following equation

$$N = 331.0e^{0.0158\ (T_{\theta a} - 100)} \qquad (5)$$

where $T_{\theta a}$ is the autohydrolysis temperature in °C. In this case R^2=0.8218 and $K = 0.00031 \pm 0.00013$ L mg^{-1} min^{-1}.

The Thomas [41] model is one of the most widely used models in the column performance theory. The main

Proc. of the Second Intl. Conf. on Advances In Bio-Informatics, Bio-Technology and Environmental Engineering- ABBE 2014.

ISBN: 978-1-63248-053-8 doi: 10.15224/ 978-1-63248-053-8-122

TABLE II. PARAMETERS AND VALUES OF SEE, WHEN NLRA IS USED, FOR THE ALTERNATIVE COLUMN MODELS CONSIDERED HEREIN.

$T_{\theta a}$	Bohart-Adams			Modified Dose-Response		
	N ($mg \cdot L^{-1}$)	K ($L \cdot mg^{-1} \cdot min^{-1}$)	SEE	q_0 ($mg \cdot g^{-1}$)	a_{mdr}	SEE
untreated	451.1	0.00024	13.091	0.6376	0.7569	2.107
160	616.0	0.00051	7.582	2.181	0.9241	4.455
200	1055.6	0.00027	7.315	7.211	1.249	1.968
240	4743.8	0.00024	2.239	23.71	2.184	1.233

difference between the Bohart-Adams and the Thomas model is the form of the sorption isotherm assumed. The latter assumes a Langmuir (favorable) isotherm. It has been shown that, when the sorption isotherm is highly favorable, the actual Thomas model reduces to the Bohart-Adams model. The expression by Thomas for an adsorption column is:

$$\frac{C}{C_i} = \frac{1}{1 + e^{k_{Th} q_e x / Q - k_{Th} C_i t}} \text{ or } \frac{C}{C_i} = \frac{1}{1 + Ae^{-bt}} \quad (6)$$

where $A=k_{Th}q_e x/Q$ and $b=k_{Th}C_i$, $q_0=NEx/m$=maximum solid-phase concentration of the solute (mg/g), $q_e=EN$, $k_{Th}=K$, $V=Qt$=volume of metal solution passed into the column (L), E=cross-section of the column (cm^2), Q=flow-rate (L min^{-1}), m=adsorbent mass (g). It can be seen that the Thomas model equation can be transformed the Bohart-Adams model.

The Yoon–Nelson [42] model is not only more simplified than the other models, but, also, it does not require detailed data concerning the characteristics of adsorbate, the type of adsorbent, and the physical properties of the adsorption bed. Evidently, the Yoon-Nelson model can be transformed to the Bohart-Adams model. The Yoon–Nelson model equation for a single component system is expressed as:

$$\frac{C}{C_i} = \frac{e^{k_{YN} t - \tau k_{YN}}}{1 + e^{k_{YN} t - \tau k_{YN}}} \text{ or } \frac{C}{C_i} = \frac{1}{1 + Ae^{-bt}} \quad (7)$$

where k_{YN} is the rate constant (min^{-1}), τ the time required for 50% adsorbate breakthrough (min) and t is the breakthrough/sampling time (min). $A = e^{k_{YN} \tau}$ and $b=k_{YN}$.

The Modified Dose–Response (MDR) model was proposed by Yan *et al.* [43, 44] because it minimizes the error resulting from the use of the Thomas model, especially at lower and higher time periods of the breakthrough curve. The MDR model is expressed as:

$$\frac{C}{C_i} = 1 - \frac{1}{1 + \left[C_i V / (q_0 m)\right]^{a_{mdr}}} \quad (8)$$

where $b_{mdr}=(q_0 m)/C_i$ and α_{mdr} are the modified dose–response constants. The experimental data and the simulation results are given in Fig. 5. The fitting of the MDR model was much more satisfactory compared to the Bohart-Adam model. More specifically, for autohydrolysis time equal to 50 min, it was found that:

$$q_0 = 0.5624 \ e^{0.0259 \ (T_{\theta a} - 100)} \quad (9)$$

where $T_{\theta a}$ is the autohydrolysis temperature in ^oC and R^2=0.9903. In this case

$$a_{mdr} = 0.6784 \ e^{0.0073 \ (T_{\theta a} - 100)} \quad (10)$$

where R^2=0.8989.

In view of the above the adsorption capacity of autohydrolyzed Scots pine sawdust for Cr(VI) is satisfactory, rendering this low cost material suitable as an alternative to commercial activated carbons for the removal of chromium from water/wastewater effluents. Autohydrolysis may become a cost-effective method, since the pretreatment expenses are covered by the produced fermentable sugars for the bioethanol production industry, which is subsidised in the EU Countries. Furthermore, as sawdust is an industrial waste and no addition of chemicals is required, this process of adsorbent modification may be considered to take place within an 'Industrial Ecology' framework, since a solid waste is used to treat an aquatic waste, contributing to pollution abatement without entailing excessive cost [31, 32].

IV. Conclusions

Column kinetics of Cr(VI) adsorption on autohydrolyzed pine sawdust were successfully simulated, and the autohydrolysis conditions as regards time and temperature were optimized. The MDR adsorption column capacity q_0 increased 37 times, indicating the impressive effectiveness of autohydrolysis pretreatment on Cr(VI) adsorption by sawdust. The optimal autohydrolysis conditions are 240^{o}C for 50 min.

Acknowledgment

Financial support by the Research Centre of the University of Piraeus is kindly acknowledged.

References

[1] M. Bansal, D. Singh, and V.K. Garg, "A comparative study for the removal of hexavalent chromium from aqueous solution by agriculture wastes' carbons," J. Hazard. Mater., vol. 171, pp. 83-92, 2009.

[2] D. Mohan, S. Rajput, V. K. Singh, P. H. Steele, and C. U. Pittman, "Modeling and evaluation of chromium remediation from water using low cost bio-char, a green adsorbent," J. Hazard. Mater., vol. 188, pp. 319-333, 2011.

[3] V.K. Gupta, P.J.M. Carrott, M.M.L. Ribeiro-Carrott, and Suhas, "Low-Cost Adsorbents: Growing Approach to Wastewater Treatment - a Review," Crit. Rev. Env. Sci. Tec., vol. 39, pp. 783-842, 2009.

[4] S.J. Allen, Q. Gan, R. Matthews, and P.A. Johnson., "Comparison of optimised isotherm models for basic dye adsorption by kudzu," Biores. Technol., vol. 88(2), pp. 143-152, 2003.

[5] F.A. Batzias, and D.K. Sidiras, "Dye adsorption by calcium chloride treated beech sawdust in batch and fixed-bed systems," J. Hazard. Mater., vol. B114, pp. 167-174, 2004.

ISBN: 978-1-63248-053-8 doi: 10.15224/ 978-1-63248-053-8-122

[6] A. Sohail, S.I. Ali, N.A. Khan, and R.A.K. Rao, "Extraction of chromium from wastewater by adsorption," Environ. Pollut. Control. J., vol.2, pp.27-31, 1999.

[7] D. Mohan, and Ch.U. Pittman Jr, "Activated carbons and low cost adsorbents for remediation of tri- and hexavalent chromium from water," J. Hazard. Mater., vol.137, pp. 762-811, 2006.

[8] S. Kuo, and R. Bembenek, "Sorption and desorption of chromate by wood shavings impregnated with iron or aluminum oxide," Bioresource Technol., vol. 99, pp. 5617-5625, 2008.

[9] S.S. Baral, S.N. Das, and P. Rath, "Hexavalent chromium removal from aqueous solution by adsorption on treated sawdust," Biochem. Eng. J., vol. 31(3), pp. 216-222, 2006.

[10] K.M.S. Sumathi, S. Mahimairaja, and R. Naidu, "Use of low-cost biological wastes and vermiculite for removal of chromium from tannery effluent," Bioresour. Technol. vol. 96, pp.309-316, 2005.

[11] M.H. Isa, N. Ibrahim , H.A. Aziz, M.N. Adlan , N.H.M. Sabiani , A.A.L. Zinatizadeh, and S.R.M. Kutty, "Removal of chromium (VI) from aqueous solution using treated oil palm fibre," J. Hazard. Mater., vol. 152 , pp.662-668, 2008.

[12] H. Demiral, İ. Demiral, F. Tümsek, and B. Karabacakoğlu, "Adsorption of chromium(VI) from aqueous solution by activated carbon derived from olive bagasse and applicability of different adsorption models," Chem. Eng. J., vol. 144(2) , pp.188-196, 2008.

[13] R. Chand, T.Watari, K. Inoue, T. Torikai, and M. Yada, "Evaluation of wheat straw and barley straw carbon for Cr(VI) adsorption," Sep. Purif. Technol ., vol. 65, pp. 331-336, 2009.

[14] G. Moussavi, and B. Barikbin, "Biosorption of chromium (VI) from industrial wastewater onto pistachio hull waste biomass," Chem. Eng. J., vol. 162 , pp. 893-900, 2010.

[15] D.C. Sharma, and C.F. Forster, "A comparison of the sorbtive characteristics of leaf mould and activated carbon columns for the removal of hexavalent chromium," Process. Biochem., vol. 31 (3), pp.213-218, 1996.

[16] K.K. Singh S.H. Hasan M. Talat V.K. Singh, and S.K. Gangwar, "Removal of Cr (VI) from aqueous solutions using wheat bran," Chem. Eng. J.vol. 151, pp.113-121, 2009.

[17] X. Xu, B.Y Gao, X. Tang, Q.Y. Yue, Q.Q.Zhong, and Q. Li, "Characteristics of cellulosic amine-crosslinked copolymer and its sorption properties for Cr(VI) from aqueous solutions," J. Hazard. Mater. vol. 189, pp. 420-426, 2011.

[18] E. Pehlivan, and T.Altun, "Biosorption of chromium (VI) ion from aqueous solution using walnut, hazelnut and almond shell," J. Hazard. Mater. vol.155, pp. 378-384, 2008.

[19] X.S. Wang, Z.Z. Li, and S.R. Tao, "Removal of chromium (VI) from aqueous solution using walnut hull," J. Environ. Manag., vol. 90, pp.721-729, 2009.

[20] E.A. Oliveira, S.F. Montanher, A.D. Andrade, J.A. Nobrega, and M.C. Rollemberg., "Equilibrium studies for the sorption of chromium and nickel from aqueous solutions using raw rice bran," Process. Biochem., vol. 40, pp. 3485-3490, 2005.

[21] W.E. Marshall, and L.H. Wartelle, "An anion exchange resin from soybean hulls," J. Chem. Technol. Biotechnol., vol. 79, pp.1286, 2004.

[22] V. Sarin, K.K. Pant, "Removal of chromium from industrial waste by using eucalyptus bark," Bioresour. Technol., vol.97 , pp.15-20, 2006.

[23] G.S. Agarwal, H.K. Bhuptawat, and S. Chaudhari, "Biosorption of aqueous chromium(VI) by Tamarindus indica seeds," Bioresour.Technol., vol. 97 pp. 949-956, 2006.

[24] P.A. Kumar, and S. Chakraborty. "Fixed-bed column study for hexavalent chromium removal and recovery by short-chain polyaniline synthesized on jute fiber," J.Hazard. Mater., vol. 162, pp.1086-1098,2009.

[25] E. Malkoc, and Y. Nuhoglu. "Fixed bed studies for the sorption of chromium(VI) onto tea factory waste," Chem. Eng. Sci., vol.61, pp.4363-4372, 2006.

[26] X. Jimg, Y. Cao, X. Zhang, D. Wang, X. Wu, and H. Xu, "Biosorption of chromium (VI) from simulated using cationic surfactant modified spent mushroom," Desalination, vol.269, pp.120-127, 2011.

[27] G. Blázquez, F. Hernáinz, M. Calero, M.A. Martín-Lara, and G. Tenorio, "The effect of pH on the biosorption of Cr (III) and Cr (VI) with olive stone," Chem. Eng. J., vol. 148, pp. 473-479,2009.

[28] N. Mosier, C. Wyman, B. Dale, R. Elander, Y.Y. Lee, M. Holtzapple, and M. Ladisch, "Features of promising technologies for pretreatment of lignocellulosic biomass," Bioresour. Technol., vol.96, pp. 673-686, 2005.

[29] D. Nabarlatz, A. Ebringerová, and D. Montané, "Autohydrolysis of agricultural by-products for the production of xylo-oligosaccharides," Carbohyd. Polym., vol. 69, pp. 20-28, 2007.

[30] D.Sidiras, F. Batzias, R. Ranjan, and M. Tsapatsis, "Simulation and optimization of batch autohydrolysis of wheat straw to monosaccharides and oligosaccharides," Bioresour. Technol., vol. 102, pp. 10486-10492, 2011.

[31] D. Sidiras, F. Batzias, E. Schroeder, R. Ranjan, and M. Tsapatsis, "Dye adsorption on autohydrolyzed pine sawdust in batch and fixed-bed systems," Chem. Eng. J., vol. 171, pp.883-896, 2011.

[32] D. Sidiras, D. Politi, F. Batzias, and N. Boukos, "Efficient removal of hexavalent chromium from aqueous solutions using autohydrolyzed Scots Pine (*Pinus Sylvestris*) sawdust as adsorbent." Int. J. Environ. Sci. Tech., vol. 10, pp. 1337-1348, 2013.

[33] L. Segal, J.J. Greely, A.E. Martin, and C.M. Conrad, "An empirical method for estimating the degree of crystallinity of native cellulose using the x-ray diffractometer," Textile. Res. J., vol. 29, pp.786-795, 1959.

[34] J.F. Saeman, J.F. Bubl, and E.E. Harris, "Quantitative saccharification of wood and cellulose," Ind. Eng. Chem. Anal. Ed., vol. 17 ,pp. 35-37,1945.

[35] Tappi Standards, Tappi Tests Methods, T222 om-88, Atlanta, 1997.

[36] DIN 66132, Determination of specific surface area of solids by adsorption of nitrogen; single-point differential method according to Haul and Dümbgen, 1975.

[37] Z. Wang, J. Cao, and J. Wang, "Pyrolytic characteristics of pine wood in a slowly heating and gas sweeping fixed-bed reactor," J. Anal. Appl. Pyrol., vol 84, pp. 179-184, 2009.

[38] A. Ahmad, M. Rafatullah, O. Sulaiman, M.H. Ibrahim, and R. Hashim, "Scavenging behaviour of meranti sawdust in the removal of methylene blue from aqueous solution," J. Hazard. Mater. vol. 170, pp. 357-365, 2009.

[39] G. Bohart, and E.N. Adams, "Some aspects of the behavior of charcoal with respect to chlorine," J. Am. Chem. Soc., vol. 42 ,pp. 523-544,1920.

[40] R.M. Clark, "Modeling TOC removal by GAC: The general logistic function," J. Am. Wat. Works Assoc. vol. 79, pp.33-131,1987.

[41] H.C. Thomas, "Heterogeneous ion exchange in a flowing system," J. Am. Chem .Soc. vol. 66, pp. 1664-1666, 1994.

[42] Y.H. Yoon and J.H. Nelson, "Aplication of gas adsorption kinetics. I. A. theoretical model for respiration cartridge service time," Am. Ind. Hyg. Asscoc.J., vol. 45, pp. 509-516, 1984.

[43] G. Yan, T. Viraraghavan, and M. Chen, "A new model for heavy metal removal in a biosorption column," Adsorpt. Sci. Technol. vol. 19, pp.25-43, 2001.

[44] S.V. Gokhale, K.K Jyoti, and S.S. Lele, "Modeling of chromium(VI) biosorption by immobilized Spirulina platensis in packed column," J. Hazard. Mater. vol. 170, pp. 735-743, 2009.

Assoc. Prof. D. Sidiras, BSc and PhD in chemical engineering. Teaching at the Dep. Industrial Management & Technology, Univ. Piraeus. Scopus: 39 papers, 474 citations, h-index=10.

D. Politi, PhD Student, Dep. Industrial Management & Technology, Univ. Piraeus.